JOURNAL OF MOLECULAR CATALYSIS B-ENZYMATIC (ISSN: 1381-1177) 123: pp. 81-90. (2016)

doi:10.1016/j.molcatb.2015.11.006

*Graphical Abstract (for review)

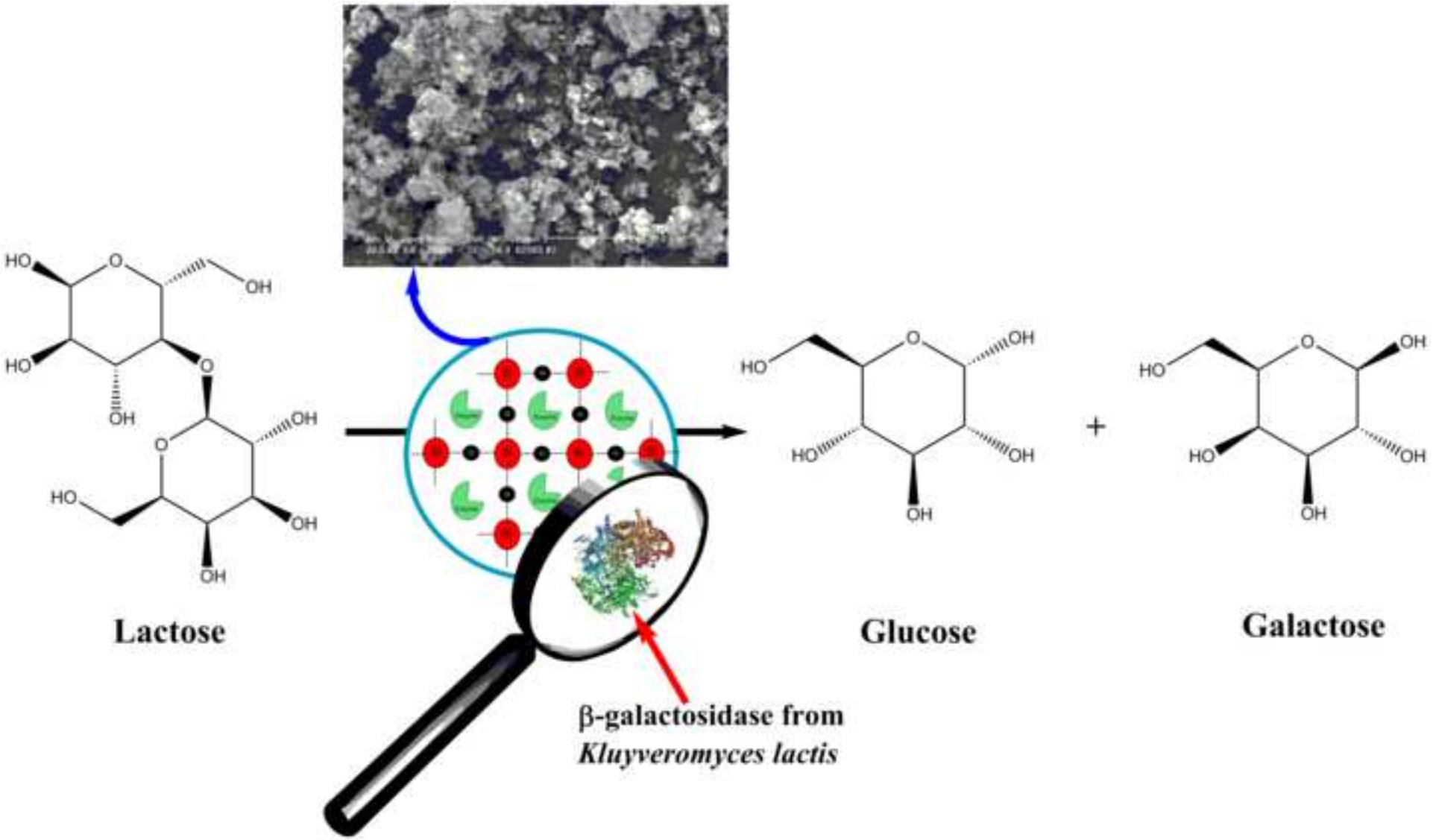

Highlights:

Alkyl substituted silane precursors were used for entrapment of β-D-galactosidase

The highest activity in optimized immobilization conditions was 84 μmol min^{-1} g^{-1}

The entrapped β-D-galactosidase demonstrated increased pH and temperature stability

More than 60% residual activity was preserved after 5 reutilizations

Recyclable solid-phase biocatalyst with improved stability by sol-gel entrapment of β-D-galactosidase

Emese Biró[a], Daniel Budugan[a], Anamaria Todea[a], Francisc Péter[a]*, Szilvia Klébert[b] and Tivadar Feczkó[b,c]

[a]Politehnica University of Timişoara, Faculty of Industrial Chemistry and Environmental Engineering, Carol Telbisz 6, 300001 Timisoara, Romania;

[b]Institute of Materials and Environmental Chemistry, Research Centre for Natural Sciences, Hungarian Academy of Sciences, Magyar Tudósok körútja 2, H-1117 Budapest, Hungary

[c]Research Institute of Chemical and Process Engineering, Faculty of Information Technology, University of Pannonia, Egyetem utca 10, H-8200 Veszprém, Hungary

*Corresponding author: Tel.: +40 256 404216; fax: +40 256 403060

E-mail address: francisc.peter@upt.ro

Abstract

β-D-galactosidase from *Kluyveromyces lactis* was for the first time immobilized by entrapment in hybrid organic-inorganic sol-gel materials with microporous structure, obtained from alkoxy silanes and alkyl substituted alkoxy silanes, in different combinations. The immobilization matrix was tailored by fine tuning of several parameters, such as: nature of alkyl group of silane precursors, molar ratio of silane precursors**,** nature of additives, protein concentration. Unlike other enzymes, β-D-galactosidase showed the best catalytic activity at low alkyl group content in the sol-gel matrix, at a molar ratio of 7:1 between the tetraalkoxysilane alkyl-trialkoxysilane precursor. The immobilized enzyme demonstrated enhanced storage, pH and thermal stability

compared to the soluble enzyme. The composite sol-gel materials were characterized by transmission electron microscopy, scanning electron microscopy, fluorescence confocal microscopy, and porosity measurement. The biocatalyst was successfully reused in five reaction cycles, maintaining more than 60% of the initial activity.

Keywords: β-D-galactosidase, sol-gel entrapment, *Kluyveromyces lactis*, immobilization, stability

1. Introduction

β-D-galactosidase (β-D-galactoside galactohydrolase, EC 3.2.1.23, commonly named as lactase) is an enzyme that catalyze the hydrolysis of β-1,4-D-galactosidic linkages. The main substrate containing such a linkage is lactose, a sugar present in milk and whey. Accordingly, the major applications of β-D-galactosidase (β-Gal) would be related to processing of lactose-containing products [1]. Manufacture of lactose-free milk and dairy products is important to allow consumption of such foods for people (especially children) with intestinal lactase deficiency, resulting in lactose intolerance [2]. Another important outcome of lactose hydrolysis is the increased sweetness and solubility of the resulting monosaccharides, which can generate new applications, especially for whey, obtained in large amount as a by-product of the cheese industry [3].

Although β-Gal has many applications in the food industry, the moderate stability of this enzyme is the main inconvenience which hindered its utilization as a biocatalyst on industrial scale. Even if protein engineering has emerged as a useful and efficient tool to tailor the biocatalyst of choice to suit the desired properties [4] and several other stabilization strategies were proposed [5], immobilization remains one of the most efficient options to improve the stability of enzymes. In the recent years, immobilization of β-Gal was the subject of numerous research works. β-D-Galactosidases of microbial origin, produced either by bacteria (*Escherichia coli*, *Bacillus*

circulans), yeast (*Kluyveromyces marxianus*, *Kluyveromyces lactis*), or fungi (*Aspergillus oryzae*) were studied. Several immobilization methods have been investigated, including adsorption on metal oxide powders [6], biospecific adsorption on concanavalin A - Celite 454 [7], aggregation and crosslinking with glutaraldehyde [8], but covalent binding on different supports was the most intensively studied. Immobilization of β-Gal from *Kluyveromyces lactis* was achieved on silica nanoparticles activated by glutaraldehyde [9] β-Gal from *Bacillus circulans* was immobilized by multipoint covalent attachment on macro-mesoporous silica supports activated with glyoxyl groups [10]. Acrylic supports holding epoxy groups, Eupergit and Sepabeads, were used for immobilization of β-Gal from *Bacillus circulans* as well, with alkaline incubation and reaction with β-mercaptoethanol or glycine as post-immobilization treatments to increase the thermal stability of the preparates [11]. Glutaraldehyde-activated chitosan was another important support, used for covalent immobilization of β-Gal from *Kluyveromyces lactis* [12] and *Kluyveromyces fragilis* [13], having the advantage of non-toxicity and biocompatibility. Multi-walled carbon nanotubes were also functionalized with glutaraldehyde in order to increase the bound enzyme amount [14]. The possible disadvantages of these methods are related with the lower mechanical resistance of the organic supports, leading to decrease of the stability of the biocatalyst, particularly at repeated use. Resistance to abrasion (for batch reactors) and flow pressure (for continuous reactors) is an important characteristic of the support material and could significantly influence the operational stability [15]. Another drawback could be the restricted mobility of the enzyme, due to the multipoint covalent bonding with the support, while in case of immobilization by adsorption the enzyme leakage is usually the main problem.

In recent years, encapsulation of enzymes in inorganic sol-gel matrices emerged as one of the most promising immobilization techniques. The fact that brought to this consequence was the

simplicity of obtaining sol-gels, the easiness of recycling, and possible stabilization of the tertiary structures of proteins by the rigid network of sol-gel [16]. Other important advantages covered by this technique are: they are nontoxic, are not rejected by biological organisms, do not change their volume in aqueous solutions or in organic solvents [17]. Moreover, the enzymatic preparations obtained by this method display increased mechanical, thermal and chemical stability, depending on the enzyme concentration, pH, ionic strength, additives used, as well as other immobilization conditions [18]. Despite these important advantages, only a few reports were published in the topic of sol-gel entrapment of β-Gal. Tetraethoxysilane (TEOS) derived network obtained by a standard protocol was employed for the sol-gel immobilization of β-Gal from *E. coli*, obtaining silica lentils with increased stability at pH < 4 and at 75°C pre-incubation temperature [19]. The same precursor and basically the same protocol was used for β-Gal from *Kluyveromyces lactis*, to obtain a monolithic gel with the highest activity at 50°C [20]. However, these studies were not carried out in order to systematically investigate the influence of various parameters that could influence the immobilization efficiency. Moreover, utilization of encapsulated β-Gal as lentils or monolithic gel is possibly only for specific applications and is not suitable for continuous utilization in packed columns, as needed for most industrial applications.

For xerogels obtained from a single precursor, like as tetraethoxysilane, it is expected to obtain a compact and uniform porous structure, with the geometry of the pore network depending on the process variables [21]. Such porous materials with tailored geometry and permeability have various applications, like as in separation processes, but realization of an appropriate matrix is much more difficult when this material is employed for entrapment of biomolecules. A more compact structure compulsorily leads to important diffusional and mass transfer limitations, particularly in case of substrates and products with higher molecular masses. Therefore, the

majority of enzyme immobilization studies in sol-gel systems were carried out with hybrid organic-inorganic sol-gel matrices, obtained from tetraalkoxysilanes and trialkoxysilanes holding organic functional groups that are not hydrolyzed during the immobilization process [16].

The aim of this work was to prepare highly stable solid phase biocatalysts by entrapment in nanostructured sol-gel matrices obtained from alkoxysilanes and silane precursors which contain covalently linked alkyl groups, determination of the immobilization parameters, as well as a detailed characterization of the most efficient biocatalyst. To the best of our knowledge, this is the first systematic study concerning the immobilization of β-Gal, approaching all important and critical elements of sol-gel entrapment particularized for this enzyme and providing a robust solid-phase biocatalyst suitable for continuous and large-scale use.

2. Materials and methods

2.1. Materials

The silane precursors dimethyldimethoxysilane (DMeDMeOS, 96%), propyltrimethoxysilane (PrTMOS, 97 %), tetraethoxysilane (TEOS, 98%) were purchased from Fluka Chemie GmbH (Buchs, Switzerland). *o*-Nitrophenyl β-D-galactopyranoside (ONPG), n-hexane (97%), isobutyl trimethoxysilane (*i*BuTMOS, 97%), methyltriethoxysilane (MeTEOS, 99%), fluorescein isothiocyanate (FITC), polyethylene glycols (PEG 4000 and PEG 20000), polyvinyl alcohol (PVA), cyclodextrin, glucose, bovine serum albumin (BSA), 4-aminoantipyrine were obtained from Sigma Aldrich (Steinheim, Germany). Methyltrimethoxysilane (MeTMOS, 98 %), isopropyl alcohol (*i*PrOH, 99.9%), sodium fluoride (NaF, 99%) *o*-phosphoric acid 85%, phenol, glucose oxidase from *Aspergillus niger* (GOD), peroxidase from horseradish (POD) were purchased from Merck (Darmstadt, Germany), while tetramethoxysilane (TMOS, 99 %) was a product of Acros Organics (Geel, Belgium). Sorbitol was from Serva (Heidelberg, Germany). Coomassie Brilliant Blue G-250 was purchased from Bio-Rad (Veenendaal, The Netherlands). β-

Gal from *Kluyveromyces lactis* (Maxilact LX 5000) was a kind gift from DSM (Delft, The Netherlands).

2.2. Activity assay of native β-Gal

The activity of β-Gal was determined based on the colorimetric method using *o*-nitrophenyl-β-D-galactopyranoside (ONPG) as artificial substrate, when ONP and D-galactose are formed in the presence of the enzyme [22].

In a 4 ml glass cuvette, 2.6 ml potassium phosphate buffer 0.02 mol/L, pH 7.5, 100 µl enzyme (100 U) and 300 µl ONPG 30 mmol/L were mixed. The absorbance was measured at 420 nm after 30 sec with an UV-VIS spectrophotometer (JASCO V530). One enzymatic unit U represents the amount of enzyme which transforms one µmol ONPG in one minute (µmol min^{-1} ml native $enzyme^{-1}$).

2.3. Protein content determination

Protein concentration was determined by using Bradford dye binding assay [23] and BSA as standard. The sample (25 µl) was mixed with 750 µl Bradford reagent and the absorbance at 595 nm was measured after 15 min of incubation at 25ºC. Calculation of the protein concentration was done using the BSA calibration curve in the range of 0-0.9 mg/ml.

The entrapped protein amount was calculated as the difference between the initial protein subjected to immobilization and the protein remained in the supernatant after immobilization.

2.4. β-Gal immobilization by sol-gel entrapment

The sol-gel entrapment protocol was based on a previously published methodology [24]. In a 4 ml glass vial β-Gal solution (600 µl, 200 U), 1M NaF (100 µl), and isopropyl alcohol (200 µl) were mixed (magnetic stirring, 600 rpm). When the influence of additives was investigated, 200 µl 4% (w/v) solution of the additive (PEG 4000, PEG 20000, PVA, β-cyclodextrin, D-glucose or sorbitol, respectively) were added to this mixture. Then the silane precursors mixture (at different

molar ratios, total amount of 6 mmol) was added and the mixing continued at room temperature until the gelation was started. Excepting the enzyme loading study, the enzyme/silane ratio was maintained in all immobilization experiments at the same value, 4.08 mg protein $mmol^{-1}$. The gel was kept 24 h at 4ºC to complete polymerization and then the bulk gel was washed to eliminate unreacted monomers and additives with Milli-Q (Millipor Corp., USA) water (10 ml), isopropyl alcohol (5 ml) and n-hexane (5 ml) and dried in a vacuum oven at 25ºC for 24 h. The sol-gel encapsulated enzyme was crushed in a mortar and kept in a closed vessel at 4ºC.

2.5. Activity measurement of sol-gel immobilized β-Gal

2.5.1. Hydrolysis of the ONPG substrate

In a 2 ml Eppendorf tube 5 mg of immobilized enzyme and 1.80 ml potassium phosphate buffer 0.02 mol/L, pH 7.5 were added and mixed for 20 min with 300 rpm, using a magnetic stirrer (Schott Instruments, Germany). The reaction was started by adding 200 µl solution of ONPG. after 10 min the absorbance at 420 nm was determined. The activity was calculated based on the amount of ONP formed calculated from the calibration curve of ONP at pH 7.5.

One enzymatic unit U represents the amount of enzyme which transforms one µmol ONPG in one minute ($\mu mol \times min^{-1} \times g^{-1}$ immobilized enzyme).

2.5.2. Hydrolysis of the lactose substrate

The hydrolysis reaction was carried out in 0.02 mol/L potassium phosphate buffer pH 7.5 at 30ºC, 300 rpm, adding 600 mmol/L lactose and 5 mg sol-gel preparate. 50 µl samples were taken hourly up to 8 hours. The amount of hydrolysed lactose was quantified as glucose release.

D-Glucose in the presence of D-galactose was measured in each sample spectrophotometrically, using the coupled enzyme assay with GOD and POD [25]. The reaction mixture consisting of 920 µl potassium phosphate buffer 0.1 mol/L pH 7.5, 160 µl phenol solution (0.128 mol/L), 160 µl 4-

aminoantipyrine solution (4AAP) (20 mmol/L), 160 µl POD (1mg/ml), 80 µl GOD (5 mg/ml), and 100 µl reaction sample was incubated at room temperature for 1 h (protected from light), then the absorbance was determined at 505 nm. Glucose concentration was determined based on a calibration curve, in the concentration range 0.5-5 mmol/L.

All experiments presented in sections 2.2 - 2.5 were performed at least in duplicate. The results are presented as mean values and the standard errors were less than 3%.

2.6. Characterization of the immobilized β-Gal

2.6.1. Scanning electron microscopy (SEM)

Dried particles were stuck onto the grid, vacuum-coated with a mixture of gold and palladium for 3 min, and examined for morphology using a Philips XL30 environmental scanning electron microscope (ESEM) instrument (The Netherlands) with an acceleration voltage of 20 kV, 25 kV, or 30 kV in backscatter and secondary electron modes.

2.6.2. Transmission electron microscopy (TEM)

Samples were crushed under ethanol and deposited onto copper grids which were covered by carbon supporting films. Microscopy data were acquired with a FEI MORGAGNI 268(D) (supplied by FEI Company, Europe Nanoport, The Netherlands) TEM used with the settings of 100 kV; W filament, top-entry; point resolution = 0.5 nm.

2.6.3. Measurement of specific surface area

Nitrogen physisorption measurements were performed at 77 K (-196°C) using a static volumetric apparatus (Quantachrome Autosorb 1C analyzer). The samples were previously degassed at 393 K (120°C) for 48 h. Nitrogen adsorption data were obtained using cc. 0.1 g of sample and successive doses of nitrogen until p/p0 = 1 relative pressure was reached. Only the nitrogen adsorption volumes up to a relative pressure of 0.1 were considered in the micropore size distribution and calculation of pore size based on Dubinin–Astakhov equation. The specific

surface area was calculated by the BET method in the range of relative pressures from 0.05 to 0.35. The mezopore-size distribution was calculated from desorption branch of the isotherms with the BJH method.

2.6.4. Protein labeling with fluorescein isothiocyanate (FITC)

β-Gal labeling with FITC was carried out in potassium phosphate buffer 0.02 mol/L pH 8.5. The glycerol has been removed by dialysis in potassium phosphate buffer for 24h and the resulted protein was concentrated by using a centrifugal filter device (Centricon PL-30, with a membrane nominal molecular weight limit (NMWL) of 30,000 Da). The coupling reaction was started by adding dropwise 600 µl of FITC (1mg/ml dissolved in dimethylformamide DMF) in the protein solution. The reaction mixture, protected from light, was incubated for 1 h at room temperature (based on PIERCE EZ-Label TM FITC Labeling Kit).

The labeled β-Gal was separated by unreacted FITC by several washes with potassium phosphate buffer 0.02 mol/L pH 8.5 using a centrifugal filter device (Centricon PL-30, with a membrane nominal molecular weight limit (NMWL) of 30,000 Da). UV-VIS spectra were collected after each washing until the FITC absorption maximum at 493 nm decreased below 0.1 absorbance units (A.U.). The protein concentration was determined by using the Bradford assay and the FITC labeled protein was immobilized in the same way as described at section 2.4. Fluorescence micrographs were registered by Leica True Confocal Scanner (Leica TCS SPE), with 10 fold spot magnitude.

2.7. Influence of enzyme loading

The correlation between the catalytic activity and the protein amount subjected to immobilization was examined by immobilizing 600 µl solution of the native enzyme with different quantities of protein varying between 25-60 mg/ml, as described in section 2.4.

2.8. Stability studies

2.8.1. pH profile of native and immobilized enzyme

The pH profile was investigated by incubating the native (200 U) or the immobilized (5 mg) enzyme in 1 ml 0.02 mol/L universal buffer, at pH ranging from 5.5 to 11. The activity was determined as described in sections 2.2 and 2.4, respectively.

2.8.2. Thermal stability of native and immobilized enzyme

Thermal stability was evaluated by incubating the native (200 U) and immobilized (5 mg) enzyme in 0.02 mol/L potassium phosphate buffer pH 7.5 at 30°C, 40°C, and 50°C. Samples were taken every 30 min up to 4 h and the activity was assayed as described at sections 2.2 and 2.4.

2.8.3. Reuse of the biocatalyst

The activity of immobilized β-Gal was determined after repeated reaction cycles. The studies were performed by using 10 mg sol-gel entrapped β-Gal and the concentrations of the artificial and natural substrates were 3 mmol/L ONPG and 60 mmol/L lactose, respectively. The activity was determined based on the product formation, ONP and D-glucose, respectively, as previously described. After each use the immobilized enzyme (sol-gel entrapped β-Gal) was separated by centrifugation for 7 min, 5000 rpm. The unreacted substrate was eliminate by several washes with a total volume of 2 ml potassium phosphate buffer 0.02 mol/L, pH 7.5, and the biocatalyst was reused in the same reaction conditions.

2.8.4. Storage stability

The storage stability was evaluated by storing the native (200 U) and immobilized enzyme for 20 days at room temperature (25°C) and at 4°C, respectively. The activities were measured at different time intervals, as described in sections 2.2 and 2.4.

3. Results and discussion

3.1. Influence of the structure of silane precursors on the activity of immobilized β-Gal

As discussed in the Introduction part, the nanostructure of the sol-gel materials obtained from alkoxysilane precursors is highly dependent on the precursor nature and the process parameters. Several reports, starting with the pioneering work of the Reetz group [23] demonstrated that the presence of organic groups in the matrix influences not only the texture and porous structure, but can also lead to specific interactions that improve the catalytic properties. However, such an interaction is extremely difficult to be predicted and the optimal silane precursor system must be found for each enzyme.

We studied the influence of the silane precursor structure on the immobilization efficiency of β-Gal by using methoxysilane precursors, ethoxysilane precursors and mixture of methoxy and ethoxysilane precursors, in different molar ratios. Tetramethoxysilane (TMOS), propyl-trimethoxysilane (PrTMOS), isobutyl-trimethoxysilane (*i*BuTMOS) and dimethyl-dimethoxysilane (DMeDMOS) were used as methoxysilane precursors, while tetraethoxysilane (TEOS) and methyl-trimethoxysilane (MeTEOS) were the employed ethoxysilane precursors. As it was expected, the activity of β-Gal was significantly affected by entrapment in sol-gel matrices obtained by different combinations of these precursors. Surprisingly, activity was not detected in any of the sol-gel immobilized β-Gal preparates obtained from methoxysilane precursors (Table 1). TMOS undergoes a more rapid hydrolysis than TEOS and results in a more compact structure. Most probably, the access of the substrate was sterically hindered following the entrapment. Utilization of a mixture of TMOS or TEOS and an alkyl trialkoxy silane as precursor leads to increased hydrophobicity of the matrix and higher alkyl group content, resulting in larger pore diameter, with a broader distribution [26]. However, precursors holding longer alkyl chains (n-butyl and isobutyl) were again not effective for the sol-gel entrapped β-Gal (data not presented in Table 1). The same inactivation effect was previously observed in case of lipases, but the increase of the alkyl group content led to a spectacular improvement of activity [27]. The different

behavior of β-Gal is probably due to structural differences between the enzymes, particularly concerning the active site. The high hydrophobicity of the matrix, which can also hinder the access of the aqueous substrate solution to the catalytic site, is another possible explanation.

The activity values presented in Table 1 were improved by the presence of TEOS as silane precursor in the sol-gel matrix formation, as the substrate access in the catalytic site of the enzyme was probably favored by the porous structure or the lower hydrophobicity of the matrix. The reactivity of TEOS in the hydrolysis and condensation reaction is not so high, consequently not all Si-OH groups formed during the hydrolysis are involved in the condensation reactions throughout the gelation process, leading to a more hydrophilic matrix.

In the next step, the possible increase of the activity of TEOS-based gels by adding silanes with covalently linked alkyl groups in the precursor mixture was investigated. Three different silane precursors, dimethyldimethoxysilane (DMeDMOS), methyltriethoxysilane (MeTEOS), and methyltrimethoxysilane (MeTMOS) were tested at 1:1 molar ratio to TEOS. Utilization of DMeDMOS and MeTEOS resulted in xerogels with lower activity compared to those based only on TEOS (Table 1, entries 5 and 6, respectively), while precursor mixtures from MeTMOS and TEOS led to inactive preparates (Table 1, entries 4 and 8, respectively). The increase of the relative amount of TEOS in the sol-gel matrices was beneficial for β-Gal immobilization efficiency (Table 1, entries 9 and 10, respectively), but a higher relative content of methyl groups had a reverse effect (Table 1, entry 7).

Based on these results that clearly demonstrated the influence of the nature and concentration of the alkyl groups incorporated in the sol-gel matrix, a systematic investigation of the silane precursor system composition was carried out, with mixtures of TEOS with DMeDMOS and MeTMOS, respectively. The results are discussed in the next section.

To investigate the effect of the nature of silane precursors on the morphology of the immobilized preparates, scanning electron microscopy (SEM) was used to provide information about the microstructure, porosity and texture of materials.

The SEM micrographs of immobilized enzymes in sol-gel matrices of methoxysilane and ethoxysilane precursors are presented in Fig. 1.

The structures can be correlated with the activity of the biocatalyst. The SEM image of the entrapped β-Gal in a sol-gel matrix obtained from methoxysilane precursors (Fig. 1a) shows that the nanoparticles are structured in large and irregular compact blocks and the enzyme is probably entrapped inside these structures. Consequently, the access of substrate to the catalytic center of enzyme is impeded, resulting the decrease or absence of the enzymatic activity. The SEM micrograph of the β-Gal entrapped in sol-gel matrix obtained from ethoxysilane precursors (Fig. 1b) shows a more porous structure, which explains the higher catalytic activity of this biocatalyst.

3.2. Enhancement of the sol-gel immobilized β-Gal catalytic efficiency by fine tuning the molar ratio of the silane precursors

The previous experiments demonstrated the efficiency of silane precursor mixtures consisted of TEOS:DMeDMOS and TEOS:MeTEOS for the immobilization of β-Gal, but also the influence of the relative content of the alkyl functional group in the matrix on the activity. Therefore, 10 immobilized preparates were obtained by gradually increase of the TEOS relative amount, in the range from 1:1 to 19:1 TEOS:DMeDMOS molar ratio. The results depicted in Fig. 2 show that the activity of the immobilized enzyme increased at higher relative amount of TEOS in the silane mixture up to 9:1 molar ratio. Consequently, the decrease of the matrix hydrophobicity was beneficial for the activity until an optimal value. At molar ratio higher then 9:1 the activity was dropped off, even though it remained higher than the activity of the preparate with only TEOS as silane precursor. It can be concluded that just a low alkyl group content has an important role in

the formation of the gel matrix due to chain elongation of the silane precursors resulting in a matrix with larger pores which allows better conformational stability of the enzyme and permits the access of the substrate to the catalytic centre. Increasing the alkyl group content above the critical value can hinder the access of water-soluble substrates to the catalytic center due to the hydrophobicity of the sol-gel matrix.

Using MeTEOS, a triethoxy silane precursor with methyl nonhydrolyzable group, a similar tendency of the activity was observed (Fig.3.). Increasing methyl group content in the sol-gel matrix resulted in higher activities up to 7:1 TEOS:MeTEOS molar ratio, but beyond this value the activity was gradually diminished, resulting an almost Gaussian profile. The main difference compared to the previously studied alkyl-holding precursor was the approx. 3 folds higher value of the activity of the immobilized enzyme, demonstrating the significant role of the structure of the silane precursor in the formation of a sol-gel matrix appropriate to confine the enzyme. Alongside the porous structure of the matrix, this difference of activities can be also explained by the higher hydrophobicity of the matrix obtained with DMeDMOS precursor. Consequently, the careful selection of the silane precursor and the fine tuning of the relative content of the hydrophobic alkyl group allowed the selection of the optimal precursor system for this enzyme. The highest activity value, 84 units/g preparate represents an excellent result.

In order to determine the morphological structure of the sol-gel immobilizates, transmission electron microscopy (TEM) was used to provide information about size and morphology of particles (Fig. 4.). The TEM images indicate the amorphous nanostructure of the sol-gel immobilizates. The data suggest the formation of nano-aggregates involving several nanoparticles that could be formed at several levels of the polymerization process in which the silica matrix is formed. Another explanation is the possibility of polymer-bridging between neighboring

particles, when the average end-to-end distance of the polymer exceeds that of the circumference of the nanoparticles, leading to the formation of these nano-aggregates.

Nitrogen adsorption-desorption isotherm of the same preparate (Fig. 5) is of type II according to the IUPAC classification albeit presence of micropores (of width <2 nm) and slight mesopores (approximate range of 2-50 nm) are unambiguous. The isotherm rises sharply at low relative pressure where the micropore filling occurs in the precapillary condensation range. The conclusion is that micropores are present along with some mesopores.

The calculated values of surface area and pore dimension are presented in Table 2.

Mesopores are present, but not in significant amount, therefore the material can be considered mainly as microporous, with an average diameter of micropores of 1.5 nm.

3.3. Influence of nature of additives on the activity of immobilized β-Gal

Several previous reports stated that the presence of an additive, mainly a polyhydroxylic compound, in the structure of the sol-gel matrix can improve the porosity of the support and the conformational flexibility of enzyme, but these results were valid particularly for lipases [28]. The effect of polyhydroxylic compounds added during the sol-gel entrapment of β-Gal was not yet investigated, but they were considered useful for other enzymes, as glucose oxidase [29] or chloroperoxidase [30]. To investigate the influence of additives on the immobilized lactase activity, six different compounds (PEG 4000, PEG 20000, PVA, β-cyclodextrin, D-glucose and sorbitol) were selected, based on their reported usefulness for sol-gel encapsulation of other enzymes. The preparates were obtained by using TEOS and MeTEOS as precursors, in 7:1 molar ratio.

As shown in Fig. 6., PEG 4000 led to the highest value of immobilized β-Gal activity, which was comparable with the activity of the additive-free sol-gel entrapped enzyme. The utilization of polyhydroxylic additives did not result in increase of the activity. The explanation is that the

commercial β-Gal from *Kluyveromyces lactis* (Maxilact LX 5000) contains approx. 50% glycerol, a common stabilizing agent for multimeric enzymes in liquid enzyme formulations, for repressing microbial growth and formation of protective shells that prevent unfolding processes. Therefore, all immobilization mixtures implicitly contained a polyhydroxylic compound (glycerol) which was involved in the sol-gel formation. Rao and Kulkani reported that addition of glycerol as drying control chemical led to narrow and more uniform pores in case of silica aerogels derived from TMOS and MeTMOS [31]. The presence additives could be important to obtain a desired pore size and improve the mechanical properties of the formed gels, but their effect on the activity is ambiguous and specific for every enzyme. As an example, glucose was found as competitive inhibitor of β-Gal from *Kluyveromyces lactis* [32]. This can explain the lower activities in presence of glucose and glucose derivatives, compared to other additives (Fig. 5). Neri et al. immobilized β-Gal from *Aspergillus oryzae* on magnetic polysiloxane-polyvinyl alcohol, thus using polyvinyl alcohol not as additive but component of the immobilization matrix [33]. Our study revealed that in the implicit presence of the glycerol from the commercial enzyme formulation, supplementary polyhydroxylic additives had no increasing effect on the activity of sol-gel immobilized β-Gal.

Although the activity was not increased, the additive had positive effect on the porous structure of the sol-gel preparate, demonstrating the dispersant properties of the additive. The SEM micrograph of the sol-gel matrix without additive (Fig. 7a) showed a less uniformly distributed structure and lower porosity than in the case of the sol-gel preparate with additive (Fig. 7b).

3.4. Influence of enzyme loading on the activity of sol-gel immobilized β-Gal

High enzyme loadings are required for application of immobilized biocatalysts in the large-scale production of industrial and consumer products. As the presence of underused biocatalyst results in lower activity, the maximum amount of enzyme that can be loaded in a support without

diffusion limitations must be determined, to ensure an optimal enzyme loading of the immobilized biocatalyst [34]. Another possible drawback at high enzyme loading could be the self-aggregation of the enzyme molecules, even if sol-gel immobilization is considered better than other encapsulation methods [19].

The optimal amount of the loaded protein was determined within the sol-gel matrix obtained from TEOS and MeTEOS, at 7:1 molar ratio, using five preparates at increasing protein concentrations, in the range of 4-10 mg protein/mmol silane (Table 3). Although the protein immobilization yield was high in all experiments, the activity was not proportionally correlated with the immobilized protein amount. The activity decreased at protein loadings higher than 100 mg g^{-1}, but the obtained values were only slightly different (less than 7%) in a relatively wide range, between 65 and 130 mg g^{-1}. Admitting that sol-gel entrapment usually prevents aggregation of the enzyme, the decline of activity at higher enzyme loading can be explained by the mentioned diffusion limitations. Nichele et al. also noticed that in the case of β-Gal immobilization in TEOS monolithic gels the best activity of the enzyme/silica gel composite was achieved at an intermediate amount of entrapped protein [20].

3.5. Reproducibility of the immobilization method

In order to evaluate the reproducibility of the immobilization method, the same procedure was performed in the same conditions, using TEOS and MeTEOS as silane precursors at 7:1 molar ratio, as described in section 2.4. The results presented in Table 4 indicate an excellent reproducibility.

The main values were 373.64 ± 4.93 mg for the mass of the encapsulated enzyme (standard deviation ± 1.32%) and 83.15 ± 1.07 U min^{-1} for the activity of the immobilized enzyme (standard deviation ± 1.30%).

3.6. Characterization and stability of the immobilized enzymes

3.6.1. pH profile of native and immobilized β-Gal

pH is one of the most important parameters for enzymatic activity, which can be inhibited at extreme pH values, because the ionic state of amino acids that form the enzyme active site could be affected. Moreover, the protein structure may suffer general unfolding leading to complete inactivation. Usually, native enzymes present activity in a narrow pH range, but this inconvenience could be improved by immobilization [35,36]. The sol-gel entrapped enzyme was more stable at higher pH values (Fig.8). A shift in optimum pH value from 7.5 to 8.0 was observed and the sol-gel entrapped β-Gal showed clearly higher activity in the pH range 8.0 - 9.0. A similar shift of the optimal activity to the basic region was reported by Song et al. when β-Gal from *Kluyveromyces lactis* was covalently immobilized on the silica gel surface by glutaraldehyde as linker [37]. Immobilization usually results in shift of optimum pH due to conformational changes in enzymes. This shift in optimum pH could result from the change in acidic and basic amino acid side chain ionization in the microenvironment around its active site. [38]. Kobayashi and Laidler [39] stated that immobilization of an enzyme does not bring any change in optimum pH when the charge on the matrix used for immobilization is nil and diffusional effects are negligible. Since sol-gel matrices do not have any charge, the shift of the optimum pH of the immobilized β-Gal by 0.5 pH units to the basic region could be assigned to diffusional effects.

3.6.2. Thermal stability of native and immobilized β-Gals

The activity of enzymes, except thermostable enzymes, is usually decreasing or is completely lost with increasing of operation temperatures, due to the irreversible conformational changes at tertiary structure level [40]. Thermal inactivation represents one of the major impediments for biocatalyst uses in industry. In several cases the thermostability of enzymes was improved by immobilization. In order to evaluate the temperature effect of immobilized enzyme, native

enzyme and sol-gel entrapped β-Gal were incubated in 0.02 mol/L potassium phosphate buffer pH 7.5 at increasing temperatures, in the 30-60°C range. Incubation time was 4h for the native enzyme, and 8 h for immobilized β-Gal. The activities, assayed for the ONPG substrate at pH 7.5, were expressed as percentage of the initial activity value. The results from Fig. 9 show that the bio-functionality of β-Gal has been improved by immobilization.

While the native enzyme at 50ºC was completely inactivated after 2 h (Fig.9a), no lost in activity was observed for the encapsulated enzyme (Fig. 9b). At 60ºC, the entrapped enzyme activity decreased only after 4 h of incubation (Fig. 9b). These results confirmed once again that encapsulation in sol-gel matrices preserve the enzymatic activity at higher temperatures and improves the thermostability. It was also demonstrated that sol-gel entrapment can led to higher thermal stability compared to adsorption or covalent binding. β-Gal from *Aspergillus oryzae* immobilized by adsorption onto native zinc oxide particles and ZnO-nanoparticles exhibited 62% and 55% of the initial activity after 2 h incubation at 60°C, respectively [41], while β-Gal from *Kluyveromyces lactis* covalently immobilized to functionalized silicone retained 47% of its initial activity after 8 h incubation at 35°C [9].

3.6.3. Distribution of the immobilized β-Gal inside the matrix

The protein labeling with FITC is based on the reaction of the isothiocyanate group with a primary amino, imidazolyl, sulfhydryl, tyrosyl or carbonyl free group from the protein structure. However, only derivatives with primary amino (e.g. lysine) groups display stability [42,43].

The distribution of the enzyme in the sol-gel matrix was evaluated by fluorescence confocal microscopy. The native protein was tagged with FITC as described in section 2.11, and the unreacted FITC was removed by several washes with potassium phosphate buffer. The labeled enzyme was immobilized by sol-gel entrapment in the same way as the non-labeled one. Confocal laser scanning microscopy was employed to display the distribution of the immobilized

β-Gal-FITC inside the sol-gel matrix (Fig. 10). The confocal images indicate a relatively uniform distribution of the enzyme, demonstrating the appropriateness of the immobilization method, but they cannot give information about the steric hindrance or conformational changes that can result in loss of activity. Control images were registered for non-labeled immobilized β-Gal, without showing any fluorescence. The fluorescence of the immobilized FITC-labeled β-Gal, subsequent to the complete removal of unreacted FITC, also demonstrates the stability of enzyme entrapment.

3.6.4. Multiple utilization of immobilized β-Gal in batch hydrolysis of ONPG and lactose

Reusability of the enzyme represents one of the main goals of enzyme immobilization, especially for cost-effective use of the enzyme in repeated batch or continuous systems.

In this study the effect of reuse on the immobilized enzyme activity was studied for ONPG hydrolysis and also for the hydrolysis of the natural substrate of β-Gal, lactose, to evaluate the catalytic performance of the immobilized product in view of a possible scaling-up. After each reutilization, the immobilized enzyme was recovered by centrifugation and used for the same reaction, in the conditions stated in section 2.12. The results, shown in Fig. 11, indicate a decrease in the enzymatic activity of sol-gel entrapped β-Gal to 70% of the initial value after the first utilization for the ONPG substrate, but no further activity decrease after the next five uses. Quite similar results were observed for the lactose substrate, about 40% activity loss after the first utilization and no further decrease after the next five uses.

Stabilization of the activity of covalently immobilized β-Gal from *Kluyveromyces marxianus* at about 40% of the initial activity for several batches in the lactose hydrolysis process was reported by other authors [44]. The loss of activity in the first reaction cycle can be assigned to several factors, most probably the loss of the enzyme that was not well entrapped, being immobilized

only by hydrogen bonding or hydrophobic interactions. Other possible explanations could be protein conformational changes or steric hindrances that result after the first reaction cycle.

3.6.5. Storage stability

This experiment was conducted to determine the storage stability of both the native enzyme (in potassium buffer, 0.02 mol/L, pH 7.5) and the sol-gel entrapped β-Gal (as powder). In order to evaluate the storage stability, two different temperatures were selected, 4ºC and 25ºC. The activity of the immobilized enzyme as well as native enzyme was determined by using ONPG as substrate after 5, 10, 15, and 20 days, respectively. These studies would help to assess the viability of the enzyme after storage.

The activity of native β-Gal decreased with 35% at 25ºC after 20 days of storage, while in case of the sol-gel entrapped enzyme more than 80 % of the initial activity was retrieved after 20 days (Fig. 12). After 20 days of storage at 4ºC the relative enzyme activity was higher than 90% for both native and immobilized β-Gal (data not presented in Fig. 12). These results are again better than other reported values, as β-Gal from *Kluyveromyces lactis*, immobilized on graphite surface by covalent binding with glutaraldehyde, and showed a residual activity of 86% after storage at 4°C for 20 days [45].

4. Conclusions

β-Gal has been successfully immobilized by sol-gel entrapment in organic-inorganic composite matrices containing covalently linked alkyl groups and it was found that enzyme is evenly distributed inside the porous matrix preventing aggregation of the biomolecules, while the microenvironment inside the matrix protects the enzyme against inactivating effects. This study resulted in nano-structured biocatalysts with high catalytic efficiency and stability.

Among several silane precursors, tetraethoxysilane and methyl-triethoxysilane at 7:1 molar ratio led to the highest activity of immobilized β-Gal, 84.03 μmol ONP min^{-1} g^{-1} at a protein loading value of 6.22 mg per mmol silane precursor.

Acknowledgments

This work was performed through the Partnerships in priority areas - PN II program, developed with the support of MEN-UEFISCDI, project no. PN-II-PT-PCCA-2013-4-0734, and was partially supported by the strategic grant POSDRU/159/1.5/S/137070 (2014) of the Ministry of National Education, Romania, co-financed by the European Social Fund-Investing in People, within the Sectorial Operational Programme Human Resources Development 2007-2013.

References

[1] A. Nath, S. Mondal, S. Chakraborty, C. Bhattacharjee, R. Chowdhury, Asia-Pacific J. Chem. Eng. 9 (2014) 330–348.

[2] P.S. Panesar, R. Panesar, R.S. Singh, J.F. Kennedy, H. Kumar, J. Chem. Technol. Biotechnol. 81 (2006) 530–543.

[3] M.G. Gänzle, G. Haase, P. Jelen, Int. Dairy J. 18 (2008) 685–694.

[4] G. Torrelo, U. Hanefeld, F. Hollmann, Catal. Letters 145 (2014) 309–345.

[5] R. Fernandez-Lafuente, Enzyme Microb. Technol. 45 (2009) 405–418.

[6] Y. Satyawali, S. Van Roy, A. Roevens, V. Meynen, S. Mullens, P. Jochems, W. Doyen, L. Cauwenberghs, W. Dejonghe, RSC Adv. 3 (2013) 24054.

[7] S.A. Ansari, Q. Husain, Food Bioprod. Process. 90 (2012) 351–359.

[8] C. Guerrero, C. Vera, E. Araya, R. Conejeros, A. Illanes, Bioresour. Technol. 190 (2015) 122–131.

[9] M.L. Verma, C.J. Barrow, J.F. Kennedy, M. Puri, Int. J. Biol. Macromol. 50 (2012) 432–7.

[10] C. Bernal, L. Sierra, M. Mesa, J. Mol. Catal. B Enzym. 84 (2012) 166–172.

[11] P. Torres, F. Batista-Viera, J. Mol. Catal. B Enzym. 83 (2012) 57–64.

[12] M.P. Klein, L.P. Fallavena, J. da N. Schöffer, M.A.Z. Ayub, R.C. Rodrigues, J.L. Ninow, P.F. Hertz, Carbohydr. Polym. 95 (2013) 465–70.

[13] D.C. Vieira, L.N. Lima, A.A. Mendes, W.S. Adriano, R.C. Giordano, R.L.C. Giordano, P.W. Tardioli, Biochem. Eng. J. 81 (2013) 54–64.

[14] S.A. Ansari, R. Satar, S. Chibber, M.J. Khan, J. Mol. Catal. B Enzym. 97 (2013) 258–263.

[15] P. Zucca, E. Sanjust, Molecules 19 (2014) 14139–14194.

[16] A.C. Pierre, Biocatal. Biotransformation 22 (2004) 145–170.

[17] A. Tomin, D. Weiser, G. Hellner, Z. Bata, L. Corici, F. Péter, B. Koczka, L. Poppe, Process Biochem. 46 (2011) 52–58.

[18] L.N. Corîci, A.E. Frissen, D.J. Van Zoelen, I.F. Eggen, F. Peter, C.M. Davidescu, C.G. Boeriu, J. Mol. Catal. B Enzym. 73 (2011) 90–97.

[19] M.C. Crescimbeni, V. Nolan, P.D. Clop, G.N. Marín, M. a. Perillo, Colloids Surfaces B Biointerfaces 76 (2010) 387–396.

[20] V. Nichele, M. Signoretto, E. Ghedini, J. Mol. Catal. B Enzym. 71 (2011) 10–15.

[21] R.F. Silva, W.L. Vasconcelos, Mater. Res. 2 (1999) 197–200.

[22] D. Cavaille, D. Combes, Biotechnol. Appl. Biochem. 22 (1995) 55–64.

[23] M.M. Bradford, Anal. Biochem. 72 (1976) 248–254.

[24] C. Zarcula, L. Corîci, R. Croitoru, A. Ursoiu, F. Peter, J. Mol. Catal. B Enzym. 65 (2010) 79–86.

[25] J.A. Lott, K. Turner, Clin. Chem. 21 (1975) 1754–1760.

[26] A. Venkateswara Rao, D. Haranath, Microporous Mesoporous Mater. 30 (1999) 267–273.

[27] M.T. Reetz, Adv. Mater. 9 (1997) 943–954.

[28] M.T. Reetz, A. Zonta, J. Simpelkamp, Biotechnol. Bioeng. 49 (1996) 527–534.

[29] F.-L. Wong, A. Abdul-Aziz, J. Chem. Technol. Biotechnol. 83 (2008) 41–46.

[30] L. De Matteis, R. Germani, M.V. Mancini, G. Savelli, N. Spreti, L. Brinchi, G. Pastori, J. Mol. Catal. B Enzym. 97 (2013) 23–30.

[31] A.V. Rao, M.M. Kulkarni, Mater. Chem. Phys. 77 (2003) 819–825.

[32] A.R. Park, D.K. Oh, Appl. Microbiol. Biotechnol. 85 (2010) 1427–1435.

[33] D.F.M. Neri, V.M. Balcão, R.S. Costa, I.C.A.P. Rocha, E.M.F.C. Ferreira, D.P.M. Torres, L.R.M. Rodrigues, L.B. Carvalho, J.A. Teixeira, Food Chem. 115 (2009) 92–99.

[34] I. Ardao, G. Alvaro, M.D. Benaiges, Biochem. Eng. J. 56 (2011) 190–197.

[35] B. Sahoo, S.K. Sahu, P. Pramanik, J. Mol. Catal. B Enzym. 69 (2011) 95–102.

[36] H.-T. Deng, Z.-K. Xu, X.-J. Huang, J. Wu, P. Seta, Langmuir 20 (2004) 10168–73.

[37] Y.S. Song, J.H. Lee, S.W. Kang, S.W. Kim, Food Chem. 123 (2010) 1–5.

[38] S. Talekar, S. Waingade, V. Gaikwad, S. Patil, N. Nagavekar, J. Biochem. Technol. 3 (2012) 349–353.

[39] T. Koyayashi, K.J. Laidler, Biotechnol. Bioeng. 16 (1974) 99–118.

[40] C. Vieille, G.J. Zeikus, Microbiol. Mol. Biol. Rev. 65 (2001) 1–43.

[41] Q. Husain, S.A. Ansari, F. Alam, A. Azam, Int. J. Biol. Macromol. 49 (2011) 37–43.

[42] A. Todea, A. Hiseni, L.G. Otten, I.W.C.E. Arends, F. Peter, C.G. Boeriu, J. Mol. Catal. B Enzym. 119 (2015) 40–47.

[43] M.C. Pinto, P. Macías, Biotechnol. Tech. 9 (1995) 481–486.

[44] M. Puri, S. Gupta, P. Pahuja, A. Kaur, J.R. Kanwar, J.F. Kennedy, Appl. Biochem. Biotechnol. 160 (2010) 98–108.

[45] Q.Z. Zhou, X. Dong Chen, J. Food Eng. 48 (2001) 69–74.

Table 1. Entrapment of β-Gal in sol-gel matrices using alkoxysilane precursors, with and without covalently linked alkyl groups

Entry	Silane precursors	Molar ratio	Activity [μmol ONP g^{-1} min^{-1}]
1	TMOS	-	0
2	TEOS	-	4.36
3	TMOS:MeTMOS	1:1	0
4	TEOS:MeTMOS	1:1	0
5	TEOS:DMeDMOS	1:1	0.09
6	TEOS:MeTEOS	1:1	3.09
7	TEOS:MeTEOS	1:2	0.20
8	TEOS:MeTMOS	2:1	0
9	TEOS:DMeDMOS	2:1	1.02
10	TEOS:MeTEOS	2:1	7.01

Table 2. Properties of the porous composite particles obtained by sol-gel encapsulation of β-Gal in a sol-gel matrix obtained from TEOS and MeTEOS silane precursors, at 7:1 molar ratio

BET surface area [m^2 g^{-1}]	Total volume of pores [cm^3 g^{-1}]	Total volume of mesopores [cm^3 g^{-1}]	Total volume of micropores [cm^3 g^{-1}]	Average diameter of micropores [nm]
320	0.435	0.37	0.14	1.5

Table 3. β-Gal immobilization at different protein amounts by using TEOS and MeTEOS as silane precursors, at 7:1 molar ratio

Protein/silane ratio[a] [mg mmol^{-1}]	Immobilization yield [%]	Protein loading[b] [mg/g]	Activity [U min^{-1}]
4.08	100	65.5	81.3
6.22	99.3	99.2	84.1
8.30	97.3	129.8	78.5
9.36	98.9	148.7	39.8
9.96	96.4	154.2	38.5

[a] the total silane amount was 6 mmol, for all experiments

[b] calculated as the ratio between the amount of the immobilized protein (protein subjected to immobilization × immobilization yield) and the amount of the dried immobilized preparation.

1 Table 4. Reproducibility of the immobilization method

Mass of the immobilized β-Gal preparate [mg]	Activity [U min^{-1}]
372.6	84.13
376.6	81.25
383.0	83.63
382.0	81.30
374.4	84.48
361.6	83.47
365.3	83.81

2

3

4

Legend of figures

Fig. 1. SEM micrographs of immobilized β-Gal, in sol-gel matrices of methoxysilane TMOS:MeTMOS 1:1 (a), and ethoxysilane TEOS:MeTEOS 2:1 (b) precursors

Fig. 2. Activity of sol-gel entrapped β-Gal at different TEOS/DMeDMOS silane precursor molar ratios

Fig. 3. Activity of sol-gel entrapped β-Gal at different TEOS/MeTEOS silane precursor molar ratios

Fig. 4. TEM micrographs of β-D-Gal immobilized in sol-gel matrix consisted of ethoxysilane TEOS:MeTEOS 7:1 precursors

Fig. 5. N_2 adsorption-desorption isotherm of β-Gal immobilized by sol-gel entrapment, using TEOS and MeTEOS as silane precursors, at 7:1 molar ratio

Fig. 6. Influence of the nature of additives on the activity of immobilized β-Gal

Fig. 7. Influence of nature of additives on the morphology of sol-gel matrix prepared from TEOS:MeTEOS silane precursors at 7:1 molar ratio (a) without additive; (b) with PEG 4000 additive

Fig. 8. pH profile of native (●) and sol-gel entrapped (▲) β-Gal.

Fig. 9. Effect of temperature on the activity of (a) native β-Gal at 30ºC, 40ºC, 50ºC, at incubation time up to 4h; (b) sol-gel entrapped β-Gal at 30ºC, 40ºC, 50ºC, 60ºC, at incubation time up to 8h.

Fig. 10. Fluorescence images of (a) the sol-gel entrapped labeled FITC-β-Gal; (b) the same preparate, at higher magnification

Fig. 11. Effect of reutilization on the activity of sol-gel entrapped β-Gal, using ONPG (●) and lactose (▲) as substrate

Fig. 12. Storage stability of native (●) and sol-gel entrapped (▲) β-Gal, at 25°C.

Figure 1

Click here to download high resolution image

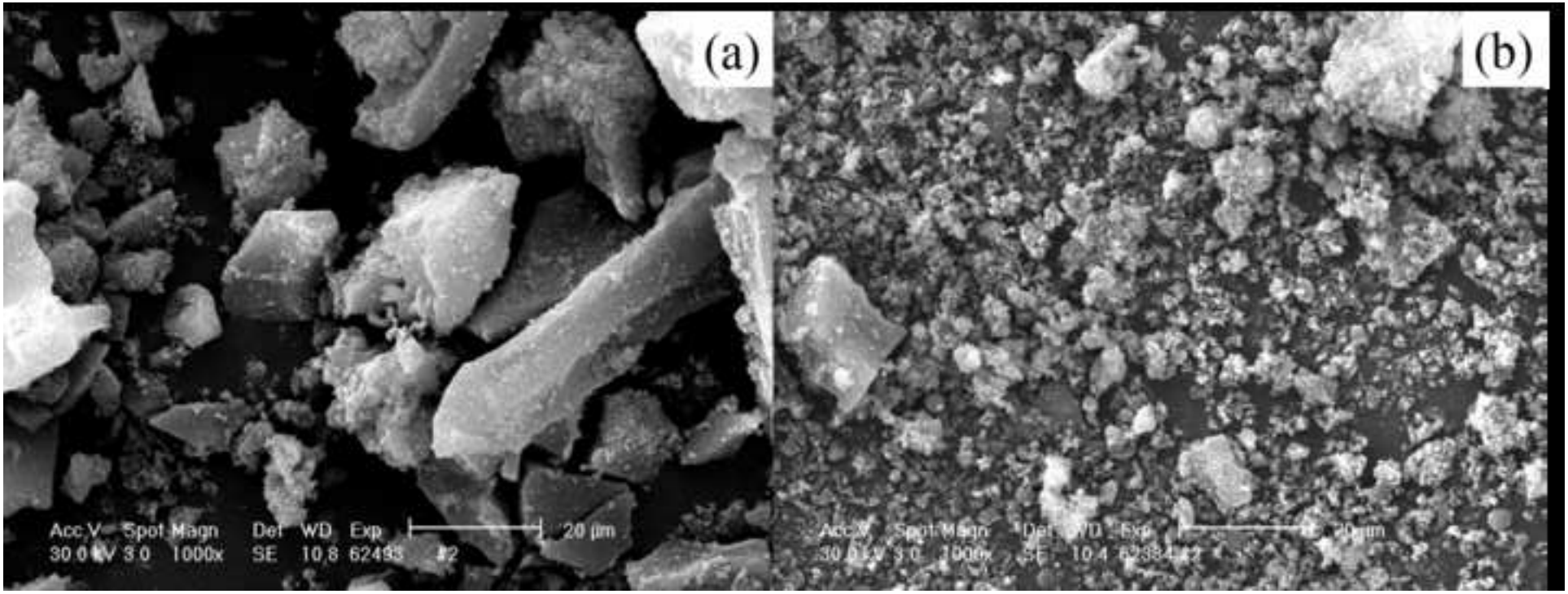

Figure 2

Click here to download high resolution image

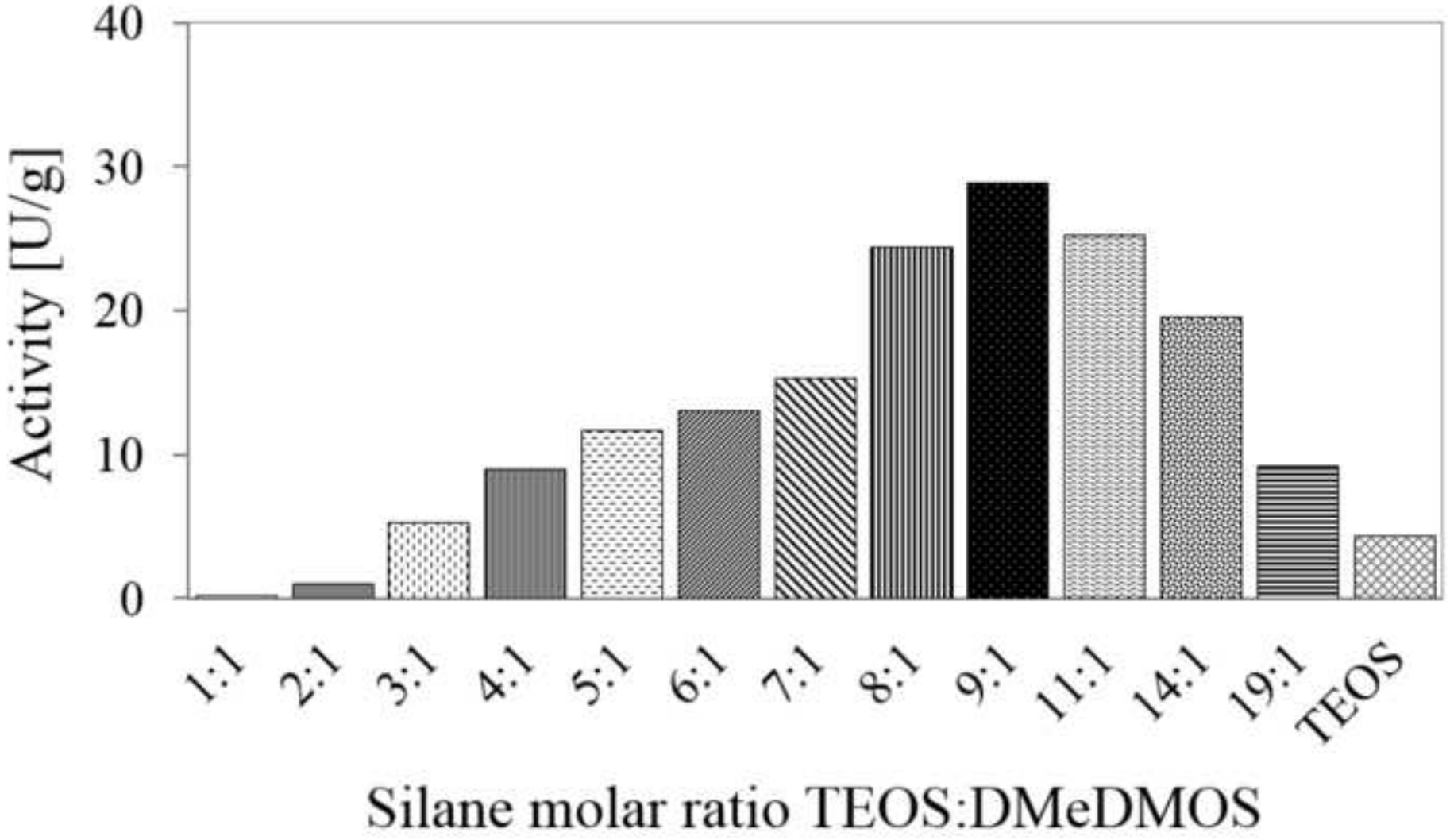

Figure 3

Click here to download high resolution image

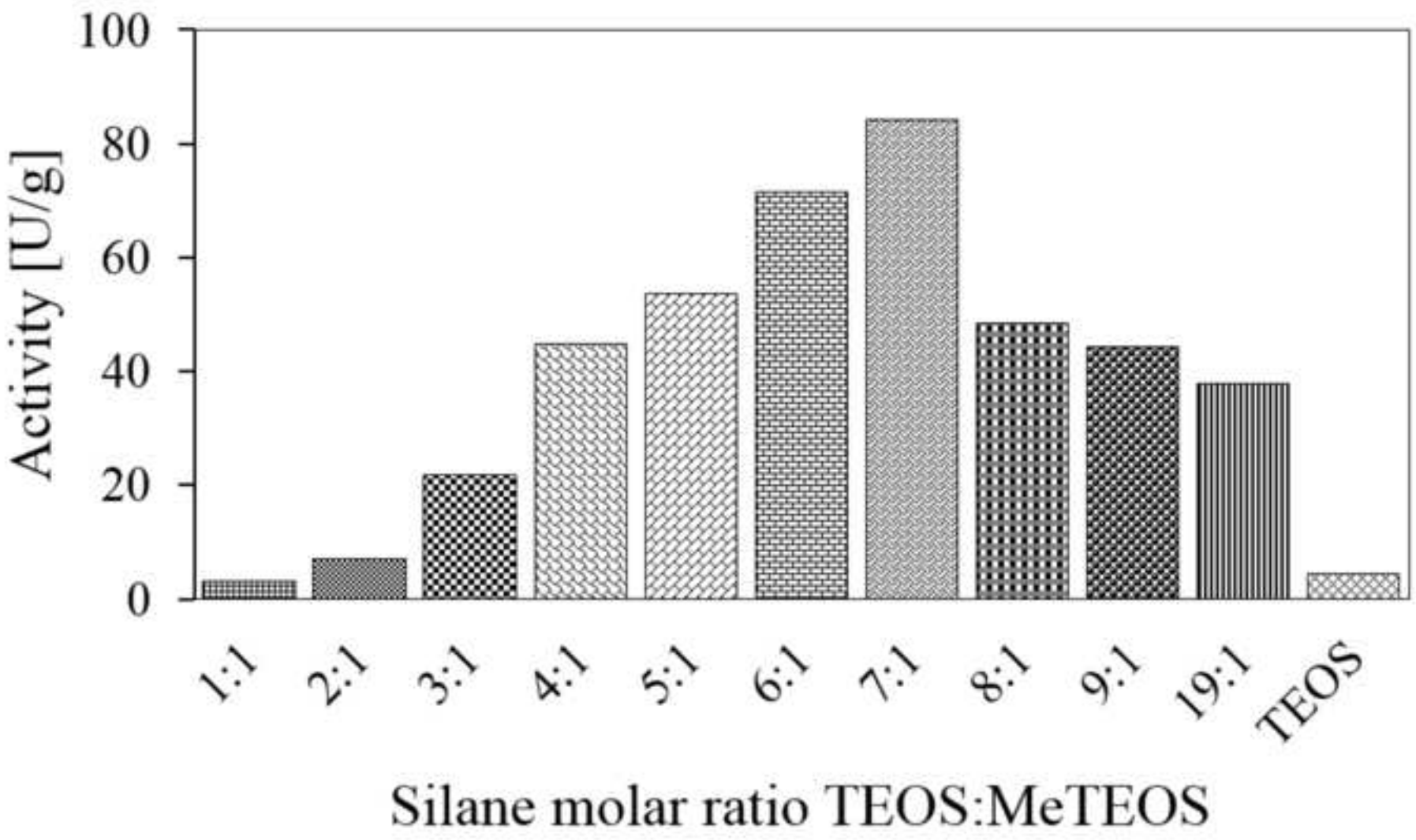

Figure 4

Click here to download high resolution image

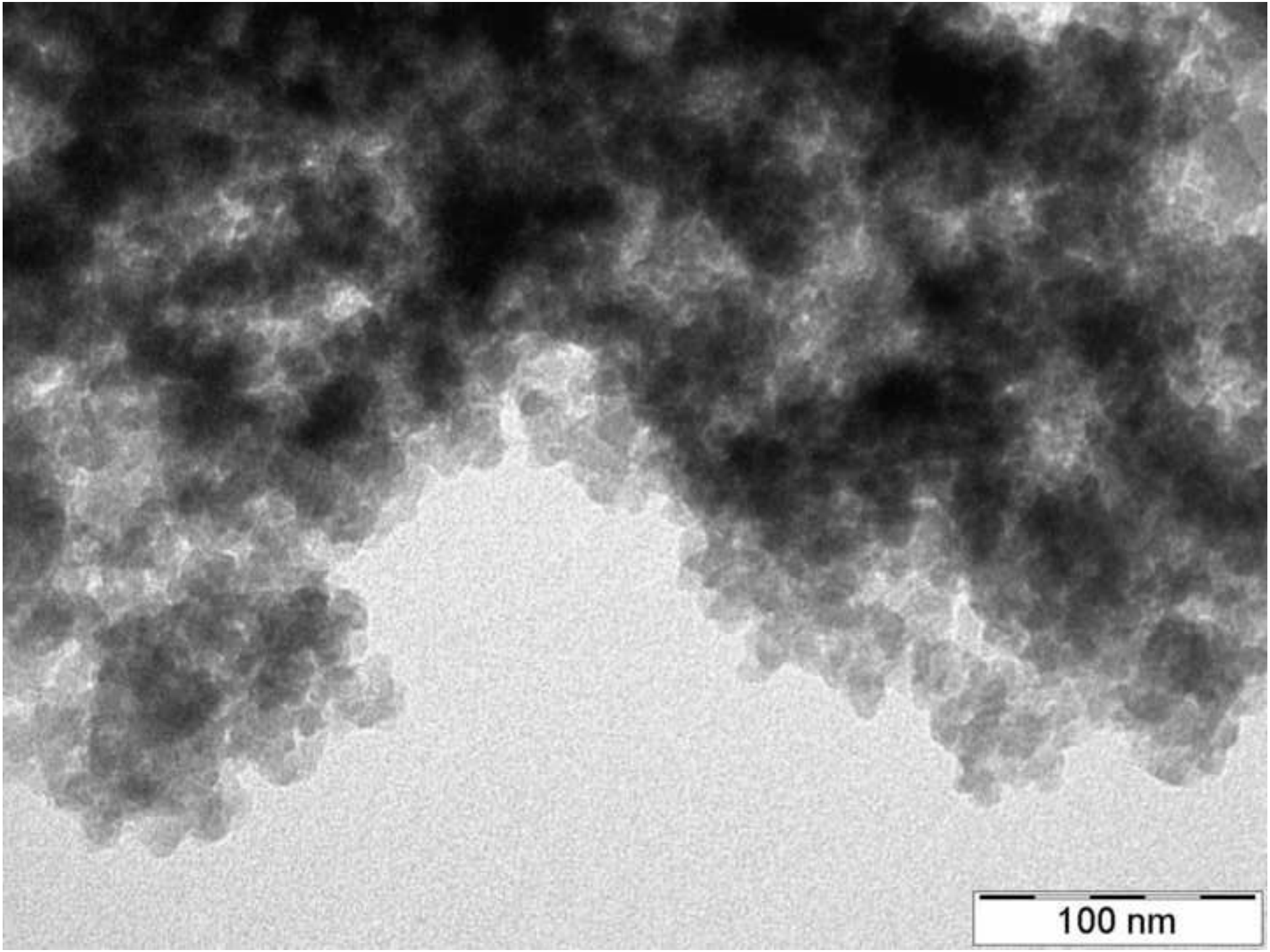

Figure 5

Click here to download high resolution image

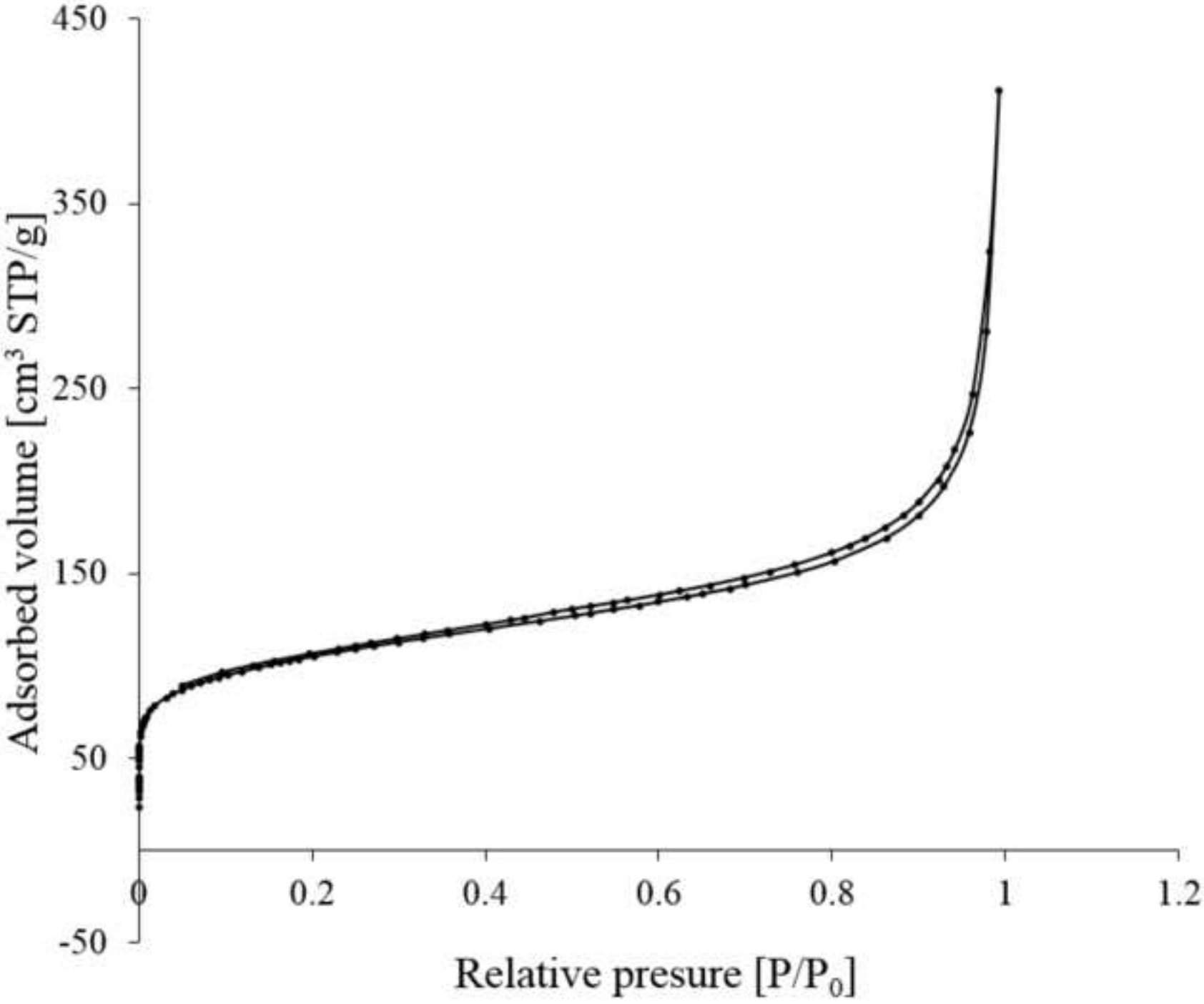

Figure 6

Click here to download high resolution image

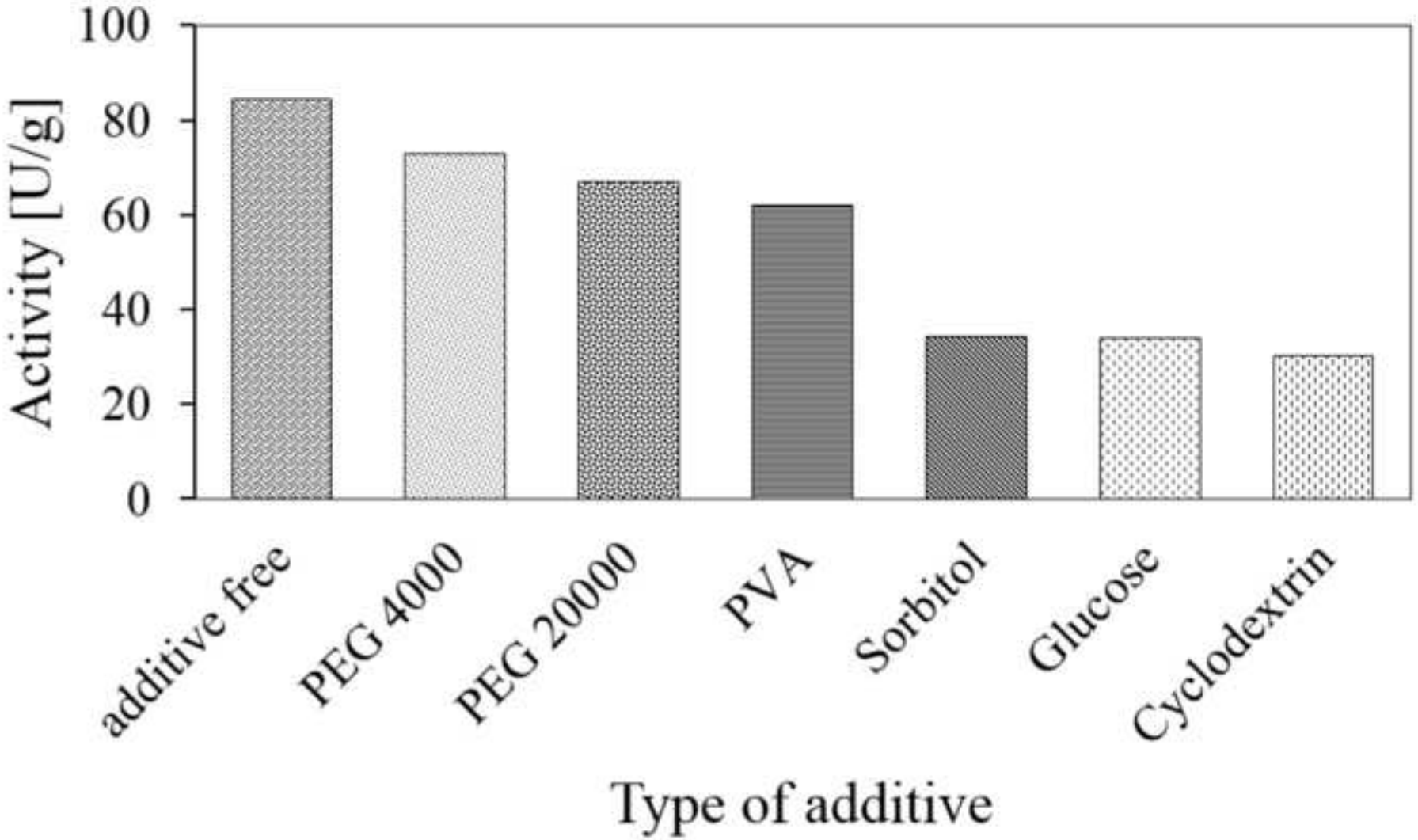

Figure 7

Click here to download high resolution image

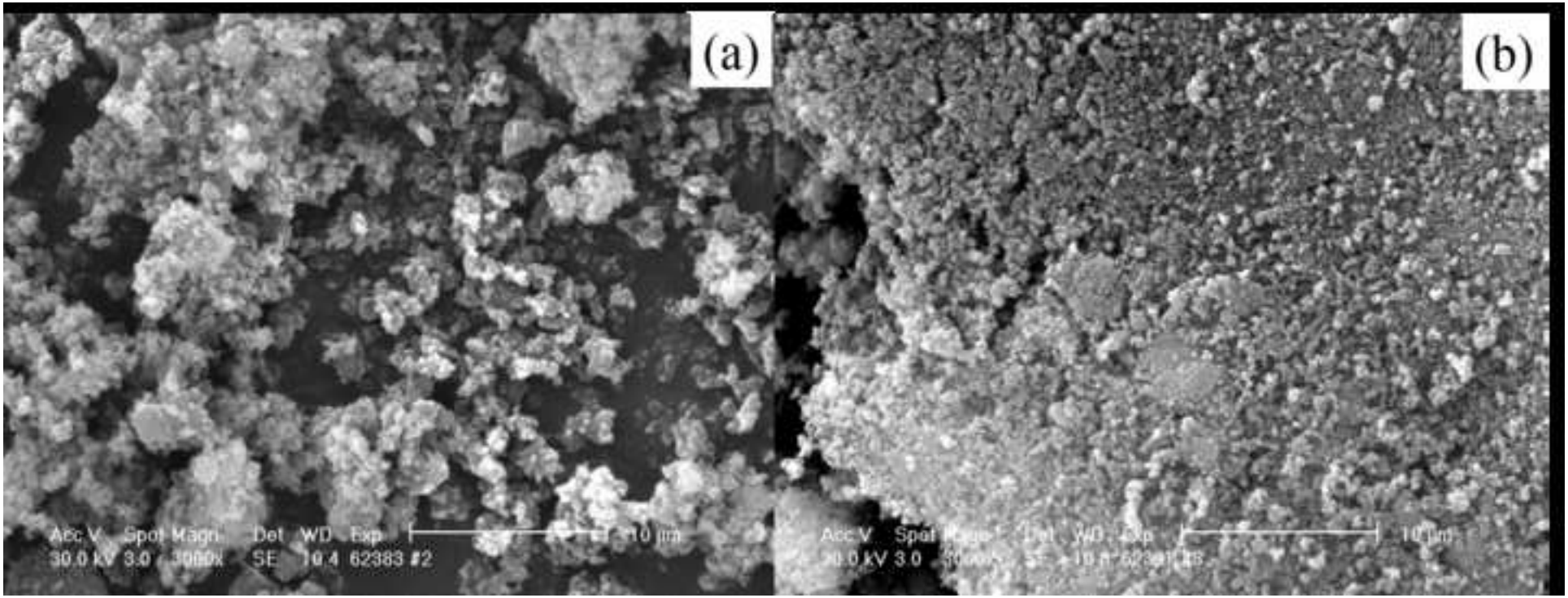

Figure 8
Click here to download high resolution image

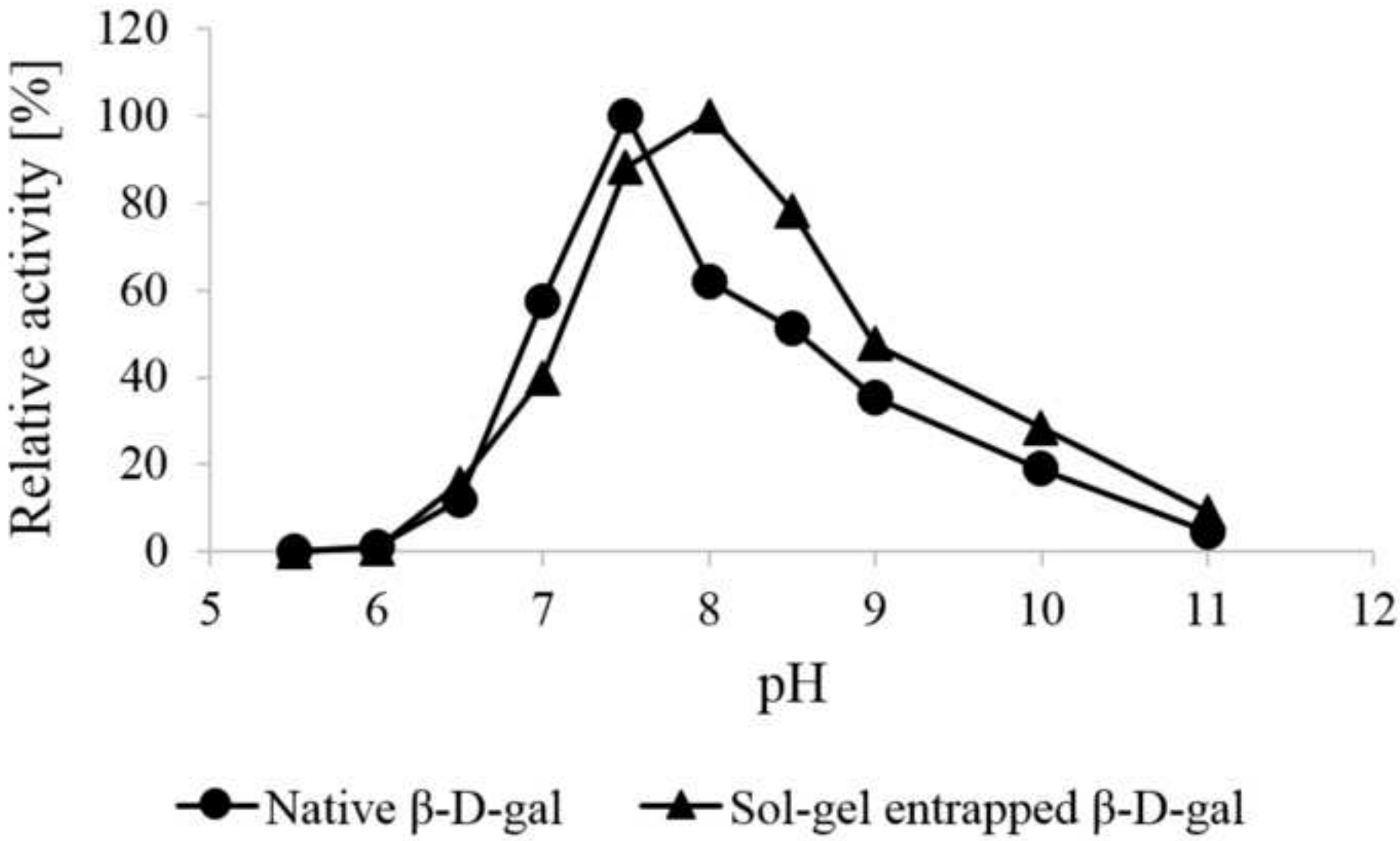

Figure 9

Click here to download high resolution image

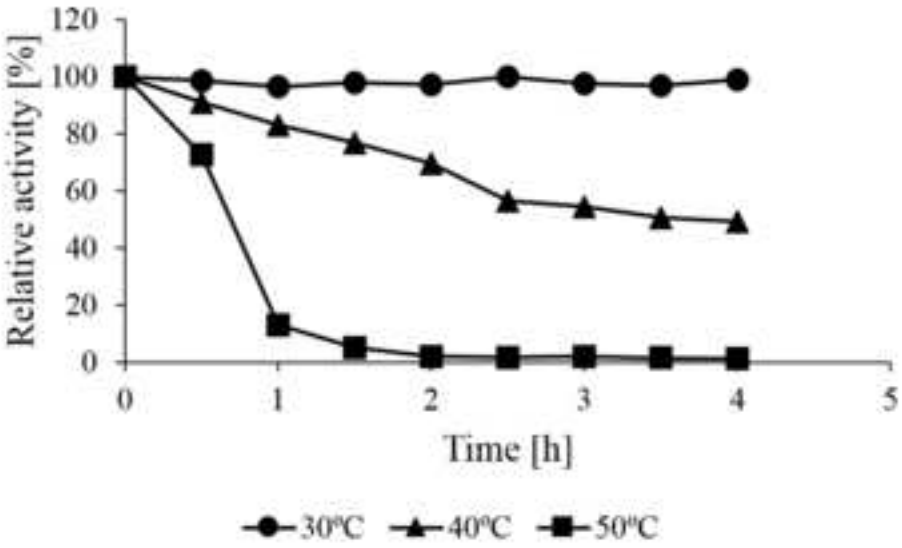

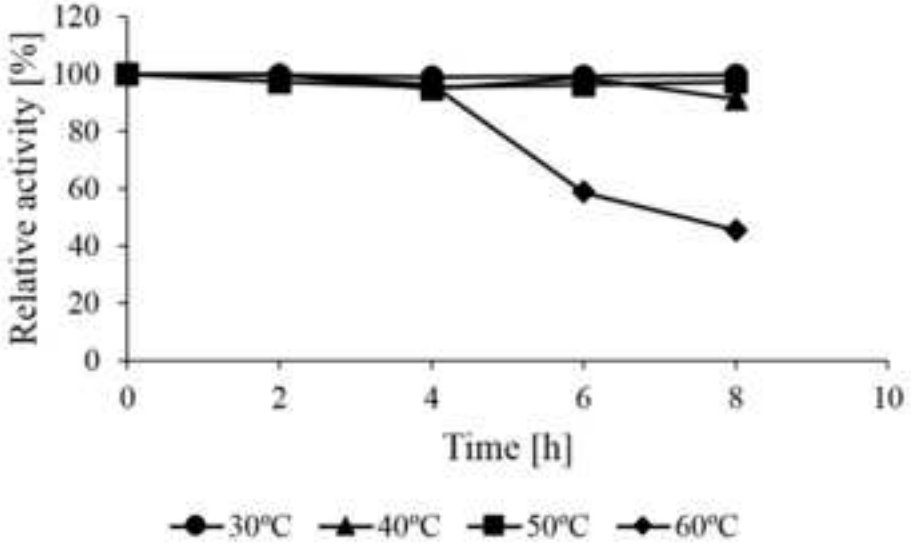

Figure 10

Click here to download high resolution image

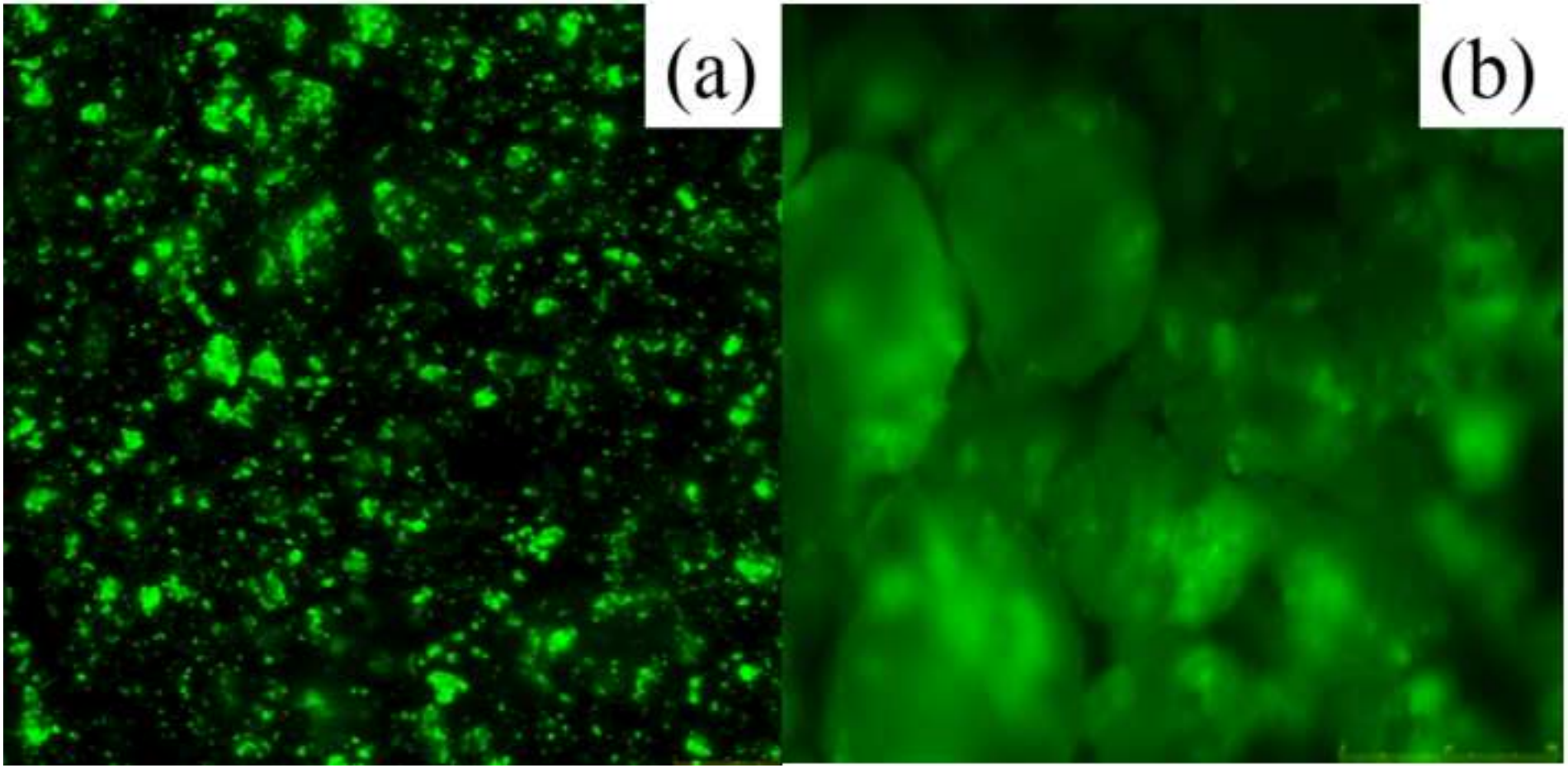

Figure 11

Click here to download high resolution image

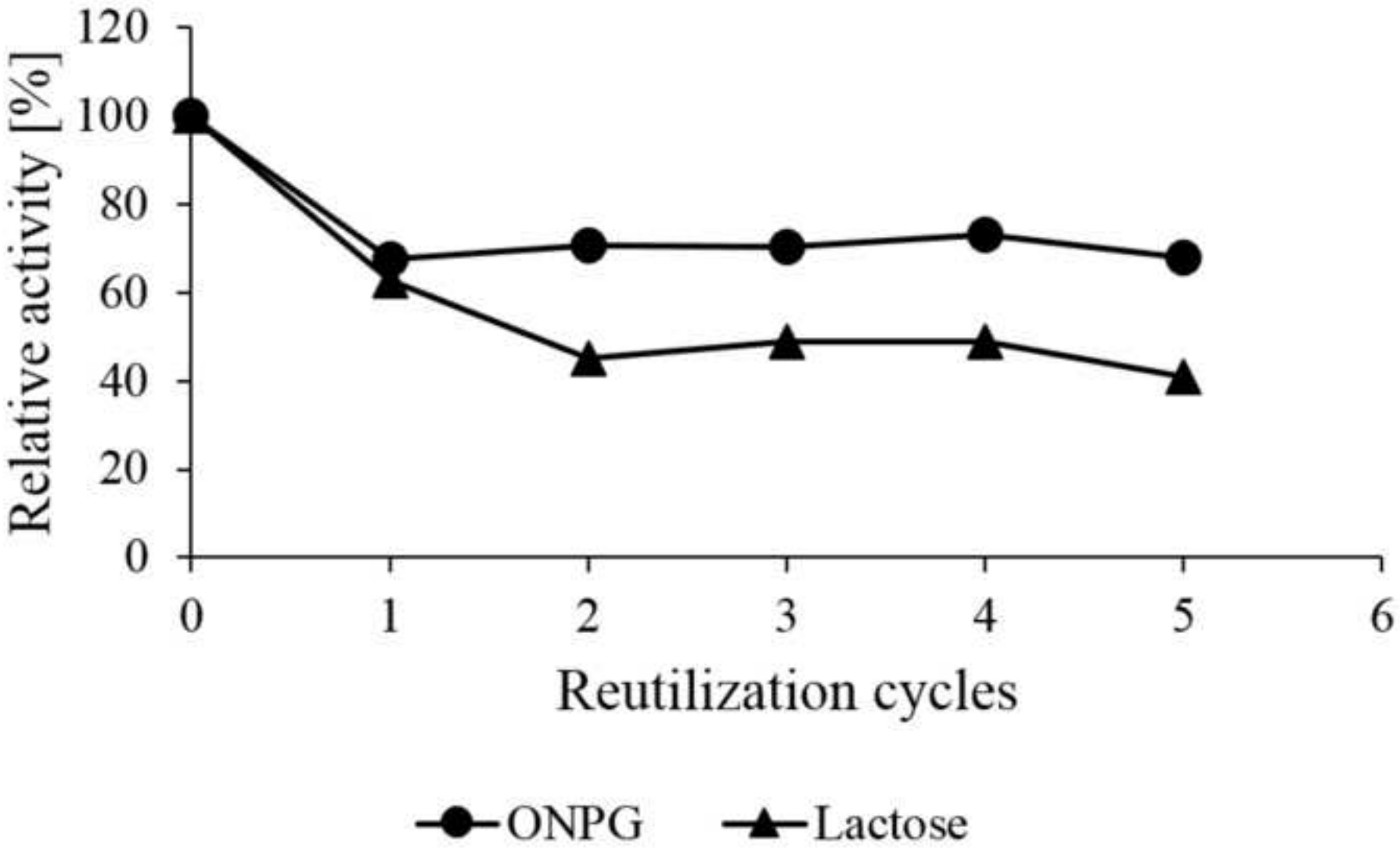

Figure 12
Click here to download high resolution image